



HAL
open science

Implicit consensus clustering from multiple graphs

Rafika Boutalbi, Lazhar Labiod, Mohamed Nadif

► **To cite this version:**

Rafika Boutalbi, Lazhar Labiod, Mohamed Nadif. Implicit consensus clustering from multiple graphs. Data Mining and Knowledge Discovery, 2021, 35 (6), pp.2313-2340. 10.1007/s10618-021-00788-y . hal-03672605v2

HAL Id: hal-03672605

<https://hal.science/hal-03672605v2>

Submitted on 24 May 2022

HAL is a multi-disciplinary open access archive for the deposit and dissemination of scientific research documents, whether they are published or not. The documents may come from teaching and research institutions in France or abroad, or from public or private research centers.

L'archive ouverte pluridisciplinaire **HAL**, est destinée au dépôt et à la diffusion de documents scientifiques de niveau recherche, publiés ou non, émanant des établissements d'enseignement et de recherche français ou étrangers, des laboratoires publics ou privés.

Implicit Consensus Clustering from Multiple Graphs

Rafika Boutalbi* · Lazhar Labiod · Mohamed Nadif

Received: date / Accepted: date

Abstract Dealing with relational learning generally relies on tools modeling relational data. An undirected graph can represent these data with vertices depicting entities and edges describing the relationships between the entities. These relationships can be well represented by multiple undirected graphs over the same set of vertices with edges arising from different graphs catching heterogeneous relations. The vertices of those networks are often structured in unknown clusters with varying properties of connectivity. These multiple graphs can be structured as a three-way tensor, where each slice of tensor depicts a graph which is represented by a count data matrix. To extract relevant clusters, we propose an appropriate model-based co-clustering capable of dealing with multiple graphs. The proposed model can be seen as a suitable tensor extension of mixture models of graphs, while the obtained co-clustering can be treated as a consensus clustering of nodes from multiple graphs. Applications on real datasets show the interest of our contribution.

Keywords Three-way data · Multiple graphs · Co-clustering · Consensus

1 Introduction

Relational data are ubiquitous in various fields (web, biology, neurology, sociology, communication, economics, etc.), and their accessibility has kept increasing in recent years. These data, as a whole, form a network formalized by a graph, where each node is an entity, and each edge is a connection between a pair of nodes; this graph can be directed or not. We find this situation in various scientific publications; the relationships between documents can often be described as multiple graphs with different types of links. In fact, several relationships, such as co-terms, co-authors, co-keywords, and

Rafika Boutalbi*
Institute for Parallel and Distributed Systems, Analytic Computing, University of Stuttgart
E-mail: rafika.boutalbi@ipvs.uni-stuttgart.de

Lazhar Labiod
Centre Borelli UMR 9010, Université Paris Cité, 75006 Paris, France
E-mail: lazhar.labiod@u-paris.fr

Mohamed Nadif
Centre Borelli UMR 9010, Université Paris Cité, 75006 Paris, France
E-mail: mohamed.nadif@u-paris.fr

co-references between documents can be used. The objective of this work is to address the clustering of multiple graphs. This is a graph mining task of clustering vertices into several groups in the presence of multiple types of proximity relations. We could hypothesize that the combination of different information that arises from multiple graphs may improve the clustering results. For instance, two documents which share a number of words and/or have one or more authors in common and/or quote each other, are likely to deal with the same topic. Incorporating this additional information leads us to consider a tensor representation of the data.

To deal with multiple graphs, various models and methods under different approaches are proposed to analyze these networks. In (Banerjee et al., 2007; Tang et al., 2009), the authors proposed a multi-way clustering framework for relational data, where different types of entities are simultaneously clustered, based not only on their intrinsic attribute values, but also on the multiple relations between the entities. Other works use a spectral decomposition-based approach relying on the combination of adjacency matrices (Tang et al., 2009; Chen et al., 2017; Nie et al., 2017). In these works, the clustering is not the main objective of the proposed approaches, nevertheless it can be deduced from decomposition results.

On the other hand, one of the most used methods in this context is the *Stochastic Block Model* (SBM) (Nowicki and Snijders, 2001) which is a probabilistic approach. SBM is commonly used for network modeling and discovering the latent community structures from a graph. It provides a statistical approach able to model data matrix, symmetric or not, into homogeneous blocks. This leads to consider SBM (Daudin et al., 2008) as a particular case of the *Latent Block Model* (LBM) proposed by Govaert and Nadif (2003, 2005) and extended in (Shan and Banerjee, 2008; Govaert and Nadif, 2013), which models any kind of data matrices not necessarily square or symmetric. In other words, the clustering of the graph directed or not, is in fact, a particular case of co-clustering. In this work, we consider graphs represented by adjacency matrices assimilated to contingency tables. Thus, considering the previous example of document clustering, the relations between documents (co-terms, co-authors, etc.) are count data and can be represented by particularly sparse contingency tables. Many works in the literature show the interest of Poisson distribution for graph theory and clustering of random graphs (Janson, 1987; Daudin et al., 2008).

To the best of our knowledge, this is the first attempt to formulate a model-based co-clustering for sparse three-way data. To this end, we rely on the latent block model (Govaert and Nadif, 2013) for its flexibility to consider any data matrices. Figure 1 presents a binary three-way dataset constructed from multiple graphs, and the expected results in terms of co-clustering. The key contributions of this work are:

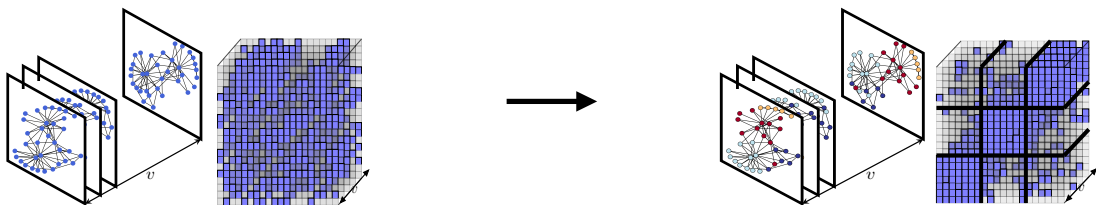


Fig. 1: Goal of co-clustering of multiple graphs.

- We first establish the links between *Poisson Latent Block Model* (PLBM) and *Poisson Stochastic Block Model* (PSBM). Then we show the interest of considering PLBM rather than PSBM.
- We propose a *Sparse* PLBM (SPLBM), a suitable probabilistic model for clustering of multiple graphs. Then we derive an EM-type learning algorithm.

- Finally, using the ensemble method, we prove that the proposed algorithm, which can be viewed as an implicit consensus clustering for multiple graphs, is more effective than explicit clustering obtained by traditional consensus clustering methods.

The remainder of this paper is organized as follows. In Section 2, we present related work and show the strong points of our approach. Section 3 reviews Poisson LBM, shows the limits of traditional PSBM and describes Sparse PLBM (SPLBM). Section 4 discusses the extension of SPLBM to consider multiple graphs. In Section 5, we present a variational Expectation-Maximization algorithm. Section 6 is devoted to evaluating our approach. Finally, section 7 concludes the paper and gives some directions for future research.

2 Related Work

Although SBM is popular in social networks analysis, dealing with the count data and due to the degree of heterogeneity, the traditional SBM fail to detect relevant clusters of edges to adress community detection problem (Qiao et al., 2017). Thereby, several authors have developed a degree-corrected SBM. In (Karrer and Newman, 2011), using a Poisson SBM, they introduced a parameter θ_i controlling the degree of expected degrees of vertices i . They consider that each x_{ij} with $i \neq j$ is distributed according to $\text{Poisson}(\theta_i \theta_j \delta_{k\ell})$, where $\delta_{k\ell}$ is the expected value of the adjacency matrix for the vertices i and j lying in block (k, ℓ) while x_{ii} is distributed according to $\text{Poisson}(\frac{1}{2} \theta_i^2 \delta_{kk})$. Doing so and under some constraints on the θ_i 's, they proposed the DC-SBM (Degree-Corrected SBM) clustering algorithm (DC-SBM¹) from an undirected graph on n vertices, possibly including self-edges. Furthermore, they established the equivalence between the maximization of the log-likelihood and the maximization of mutual information used as an objective function for clustering bipartite graphs (Dhillon et al., 2003). It is important to emphasize that the model proposed in (Karrer and Newman, 2011) is similar to that proposed by (Nadif and Govaert, 2005), where the authors also showed this connection with the maximization of mutual information; they proposed the **Croinfo** algorithm as illustrated in Figure 2. In fact, the objective function maximized by DC-SBM, which can also be used for the co-clustering of an undirected graph, is associated with a *constrained* Poisson LBM commonly used in the co-clustering context; see e.g.; (Ailem et al., 2017a,b). To sum up, considering DC-SBM which implies that the data are generated according to a Poisson LBM with $\mathcal{P}(x_{ij}, x_i, x_j, \gamma_{k\ell})$ where $\mathcal{P}(x_{ij}; \lambda) = \frac{e^{-\lambda} \lambda^{x_{ij}}}{x_{ij}!}$, the proportions of the classes of the nodes are assumed to be equal. In addition, although both algorithms DC-SBM or **Croinfo** are different, the objective is the same, and the clustering considered is based on an approach similar to that of the traditional hard clustering algorithms; for more detail, the reader can refer to recent works (Govaert and Nadif, 2013, 2018).

In our contribution, we structured graphs as three-way data where the clustering is the principal objective. We propose an extension of LBM to tackle the co-clustering of multiple undirected/directed graphs where each cell of the diagonal is not necessarily equal to an even number as conventionally considered in community detection. To do this, we adopt an EM-type approach to refer to the Expectation-Maximization algorithm (Dempster et al., 1977; McLachlan and Peel, 2000)) and not Classification EM (Celeux and Govaert, 1992). Furthermore, we will show that this purpose can be viewed as an implicit consensus clustering from Multiple Graphs.

¹ In the paper, to distinguish between a model and its derived algorithm we use *typewriter font* for an algorithm, thereby DC-SBM is the model and DC-SBM its derived algorithm.



Fig. 2: Political blogs dataset: Clustering with PSBM and DC-SBM/Croinfo.

3 Poisson Latent and Stochastic Block Models

Given an $n \times d$ data matrix $\mathbf{X} = (x_{ij}, i \in I = \{1, \dots, n\}; j \in J = \{1, \dots, d\})$, it is assumed that there exists a partition on I and a partition on J . A pair of partitions (\mathbf{Z}, \mathbf{W}) will represent a partition of $I \times J$ into $g \times m$ blocks. The partition \mathbf{Z} for rows can be represented by a label vector (z_1, \dots, z_n) where $z_i \in \{1, \dots, g\}$ or a binary matrix in $\{0, 1\}^g$ satisfying $\sum_{k=1}^g z_{ik} = 1$. In the same manner the partition \mathbf{W} for columns can be represented by a label vector (w_1, \dots, w_d) where $w_j \in \{1, \dots, m\}$ or a binary matrix in $\{0, 1\}^m$ satisfying $\sum_{\ell=1}^m w_{j\ell} = 1$.

3.1 Poisson Latent Block Model (PLBM)

Denoting \mathcal{Z} and \mathcal{W} the sets of possible labels \mathbf{Z} for I and \mathbf{W} for J , the marginal density function $f(\mathbf{X}; \Omega)$ of the *Poisson Latent Block Model* (PLBM) (Govaert and Nadif, 2018) can be written

$$f(\mathbf{X}, \Omega) = \sum_{(\mathbf{z}, \mathbf{w}) \in \mathcal{Z} \times \mathcal{W}} \prod_{i,k} \pi_k^{z_{ik}} \prod_{j,\ell} \rho_\ell^{w_{j\ell}} \prod_{i,j,k} \mathcal{P}(x_{ij}; x_i \cdot x_j \gamma_{k\ell})^{z_{ik} w_{j\ell}} \quad (1)$$

where $\Omega = (\boldsymbol{\pi}, \boldsymbol{\rho}, \boldsymbol{\gamma})$, with $\boldsymbol{\pi} = (\pi_1, \dots, \pi_g)$ and $\boldsymbol{\rho} = (\rho_1, \dots, \rho_m)$ where $(\pi_k = P(z_{ik} = 1), k = 1, \dots, g)$, $(\rho_\ell = P(w_{j\ell} = 1), \ell = 1, \dots, m)$ are the mixing proportions of row and column clusters respectively, and $\boldsymbol{\gamma} = (\gamma_{k\ell}; k = 1, \dots, g, \ell = 1, \dots, m)$. For this model, the complete data are taken to be the vector $(\mathbf{X}, \mathbf{Z}, \mathbf{W})$ where unobservable \mathbf{Z} and \mathbf{W} lead to the labels, the resulting complete data log-likelihood can be written as follows:

$$\begin{aligned} L_C(\mathbf{Z}, \mathbf{W}, \Omega) &= \log f(\mathbf{X}, \mathbf{Z}, \mathbf{W}; \Omega) \\ &= \sum_{i,k} z_{ik} \log \pi_k + \sum_{j,\ell} w_{j\ell} \log \rho_\ell + \sum_{i,j,k,\ell} z_{ik} w_{j\ell} \log \mathcal{P}(x_{ij}; x_i \cdot x_j \gamma_{k\ell}). \end{aligned}$$

To estimate Ω , we consider the EM algorithm (Dempster et al., 1977). However, the E-step using the log-likelihood of (1) directly is intractable due to the dependence structure among the rows and columns. Govaert and Nadif (2005) suggest a variational approximation in relying on the interpretation of EM due to Neal and Hinton (1998). This leads to consider the following criterion

$$L_C(\tilde{\mathbf{Z}}, \tilde{\mathbf{W}}, \Omega) + H(\tilde{\mathbf{Z}}) + H(\tilde{\mathbf{W}}) \quad (2)$$

where $L_C(\tilde{\mathbf{Z}}, \tilde{\mathbf{W}}, \Omega)$ is the fuzzy complete-data log-likelihood. $H(\tilde{\mathbf{Z}}) = -\sum_{i,k} \tilde{z}_{ik} \log \tilde{z}_{ik}$ with $P(z_{ik} = 1 | \mathbf{X}) = \tilde{z}_{ik}$, and $H(\tilde{\mathbf{W}}) = -\sum_{j,\ell} \tilde{w}_{j\ell} \log \tilde{w}_{j\ell}$ with $P(w_{j\ell} = 1 | \mathbf{X}) = \tilde{w}_{j\ell}$ are the entropies.

3.2 Poisson Stochastic Block Model

As we mentioned earlier, Poisson SBM, even DC-SBM, are particular cases of Poisson LBM insofar as the latter can model matrices, symmetric or not, oriented or non-oriented graphs, numbers of row clusters and columns clusters not necessarily equal ($g \neq m$) and finally with proportions of clusters equal or not. Therefore the transition from LBM to SBM is easy to show. Thereby, for undirected graph, the maximization of (2) leads to maximizing

$$L_C(\tilde{\mathbf{Z}}, \mathbf{\Omega}) + 2H(\tilde{\mathbf{Z}})$$

which is proportional to

$$\sum_{i,k} \tilde{z}_{ik} \log \pi_k + \frac{1}{2} \sum_{i \neq j, k \neq \ell} \tilde{z}_{ik} \tilde{w}_{j\ell} \log \mathcal{P}(x_{ij}; x_i, x_j, \gamma_{k\ell}) + \frac{1}{2} \sum_{i,k} \tilde{z}_{ik} \log \mathcal{P}(x_{ii}; x_i, x_i, \gamma_{kk}) - \sum_{i,k} \tilde{z}_{ik} \log \tilde{z}_{ik}.$$

The main differences between them are a) considering the Poisson SBM, the last term, which concerns the diagonal of \mathbf{X} , is skipped and it does not take into account the degree of nodes, unlike LBM which considers the diagonal elements. b) with Poisson LBM, $x_{ij}|z_{ik}w_{j\ell} = 1 \sim \mathcal{P}(x_i, x_j, \gamma_{k\ell})$, while with SBM $x_{ij}|z_{ik}w_{j\ell} = 1 \sim \mathcal{P}(\gamma_{k\ell})$. Notice that $\gamma_{k\ell}$ depends only on the block $k\ell$ and not on the margins. Thereby, starting from PLBM, next we will see how to take into account the sparsity often present in the graphs.

3.3 PLBM for sparse data: Sparse PLBM (SPLBM)

Recently, in (Ailem et al., 2017b), the authors proposed a generative mixture model for co-clustering document-term matrices referred to as SPLBM. With this model, they assume that for each diagonal block kk the values $x_{ij} \sim \text{Poisson}(\lambda_{ij})$ where

$$\lambda_{ij} = x_i, x_j \sum_k [z_{ik}w_{jk}] \gamma_{kk} \quad \text{or} \quad x_{ij}|z_{ik}w_{jk} = 1 \sim \mathcal{P}(x_i, x_j, \gamma_{kk})$$

and for each block $k\ell$ with $k \neq \ell$, $x_{ij} \sim \text{Poisson}(\lambda_{ij})$ where the parameter λ_{ij} takes the following form:

$$\lambda_{ij} = x_i, x_j \sum_{k, \ell \neq k} [z_{ik}w_{j\ell}] \gamma \quad \text{or} \quad x_{ij}|z_{ik}w_{j\ell} = 1 \sim \mathcal{P}(x_i, x_j, \gamma).$$

Assuming $\forall \ell \neq k, \gamma_{k\ell} = \gamma$ leads to suppose that all blocks outside the diagonal share the same parameter. SPLBM has been designed from the ground up to deal with data sparsity problems. As a consequence, in addition to seeking homogeneous blocks, it also filters out homogeneous but noisy ones due to the sparsity of the data. The pdf of SPLBM can be written as follows:

$$f(\mathbf{X}, \mathbf{\Omega}) = \sum_{(\mathbf{z}, \mathbf{w}) \in \mathcal{Z} \times \mathcal{W}} \prod_{i,k} \pi_k^{z_{ik}} \prod_{j,k} \rho_k^{w_{jk}} \prod_{i,j,k} (\mathcal{P}(x_{ij}; \lambda_{kk}))^{z_{ik}w_{jk}} \prod_{i,j,k,\ell \neq k} (\mathcal{P}(x_{ij}; \lambda))^{z_{ik}w_{j\ell}}.$$

Assuming that the complete data are $(\mathbf{X}, \mathbf{Z}, \mathbf{W})$, the complete data log-likelihood $L_C(\mathbf{Z}, \mathbf{W}, \mathbf{\Omega})$ takes the following form :

$$\log \left(\prod_{i,k} \pi_k^{z_{ik}} \prod_{j,\ell} \rho_k^{w_{jk}} \prod_{i,j,k} \left(\frac{e^{-x_i, x_j, \gamma_{kk}} (x_i, x_j, \gamma_{kk})^{x_{ij}}}{x_{ij}!} \right)^{z_{ik}w_{jk}} \prod_{i,j,k,\ell \neq k} \left(\frac{e^{-x_i, x_j, \gamma} (x_i, x_j, \gamma)^{x_{ij}}}{x_{ij}!} \right)^{z_{ik}w_{j\ell}} \right).$$

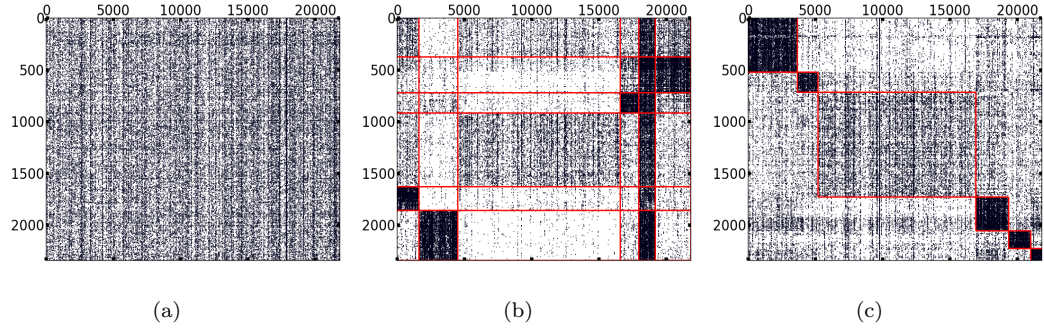


Fig. 3: (a): Original data - (b): co-clustering according PLBM - (c): co-clustering according SPLBM.

To estimate the parameters Ω , \mathbf{Z} and \mathbf{W} . To this end, a variationnel EM has been proposed (Ailem et al., 2017b) to maximize (2) where $L_C(\tilde{\mathbf{Z}}, \tilde{\mathbf{W}}, \Omega)$ is the new fuzzy complete-data log-likelihood.

Note that although SPLBM is a co-clustering model, we can derive a graph clustering algorithm from an adjacency matrix (symmetric or not). Thereby, when we are dealing with undirected graphs; strating with the same initialization of \mathbf{z} and \mathbf{w} ($\mathbf{z}^{(0)} = \mathbf{w}^{(0)}$), we obtain the same row and column clusters, that is essential for the undirected graph clustering problem.

3.4 PSBM, PLBM and SPLBM for graphs

Although PLBM can deal with sparse matrices, SPLBM can be more suitable for sparse matrices (Figure 3). It is designed to seek a diagonal block structure and capture the most reliable associations between the rows and columns object clusters. SPLBM assumes that each diagonal block (or co-cluster) is generated according to the Poisson distribution with some specific parameters, and each non-diagonal co-cluster representing noise data is generated according to Poisson distribution with identical parameters. In Figure 4 we report the graphical models of Poisson models discussed in the paper.

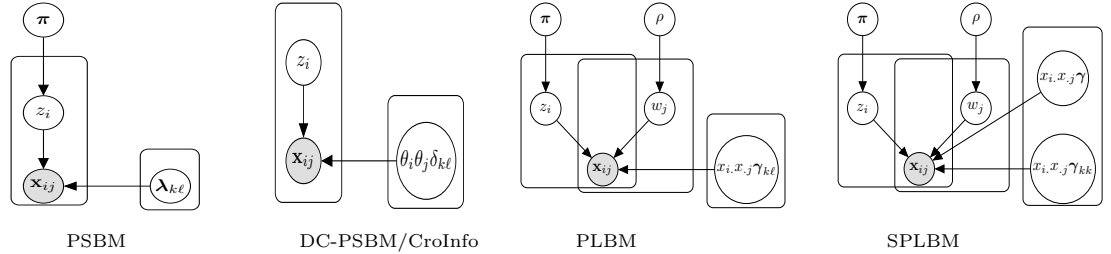


Fig. 4: Graphical models: z_i is the label of row i , w_j is the label of column j .

To clarify expectations and the impact of this parameterization, on the political blogs dataset², we applied the clustering algorithms derived from SBM, PLBM, and SPLBM, using 30 random ini-

² <https://dl.acm.org/citation.cfm?id=1134277>

tializations and measured the clustering accuracy. Figure 5 shows the interest of SPLBM, which takes into account the sparsity often present in a graph network.

The properties of this parameterization prompt us to adopt it for co-clustering with multiple graphs, as illustrated in Figure 1. Next, to avoid confusion between all the rows and columns that are identical in our case, we still keep the notations using the z_{ik} 's and $w_{j\ell}$'s.

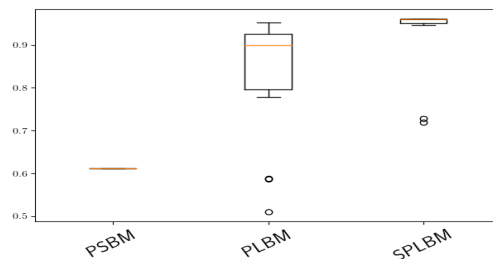


Fig. 5: Political blogs dataset: Comparison of PSBM, PLBM, and SPLBM in terms of accuracy.

The presented models PSBM, PLBM, and SPLBM deal with adjacency matrices (2D data matrix) to tackle the problem of graph clustering. In the sequel, we deal with multiple graphs organised as 3D data matrix; each matrix depicts a graph.

4 SPLBM with multiple graphs

4.1 Three-way tensor characteristics

A tensor is a multidimensional array, which is also known as the N -way, N th-order tensor. A tensor can be viewed as an element product of N vector spaces (Kolda and Bader, 2009). This notion of tensors should not be confused with tensors in physics and mathematics fields such as stress and strain tensors (Frankel, 2012).

A three-way tensor or third-order tensor has three dimensions and then has three indices, as shown in Figure 6. A first-order tensor is a vector, a second-order tensor is a matrix, and tensors of order three or higher are called higher-order tensors.

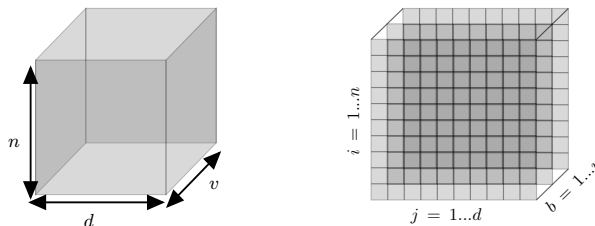


Fig. 6: Third-way tensor data representation.

The notation used here is very close to that introduced by (Kiers, 2000) for third-order tensor. Notice that scalars are represented by lowercase letters e.g. x , and vectors are expressed by a bold lowercase letter e.g. \mathbf{x} . The matrices are denoted by bold capital letters e.g. \mathbf{X} . And finally, tensors are indicated by bold capital Euler letters e.g. \mathcal{X} . The i th element of vector \mathbf{x} is denoted as x_i , the element (i, j) of a matrix is expressed by x_{ij} , and x_{ij}^b represents the element (i, j, b) of a tensor.

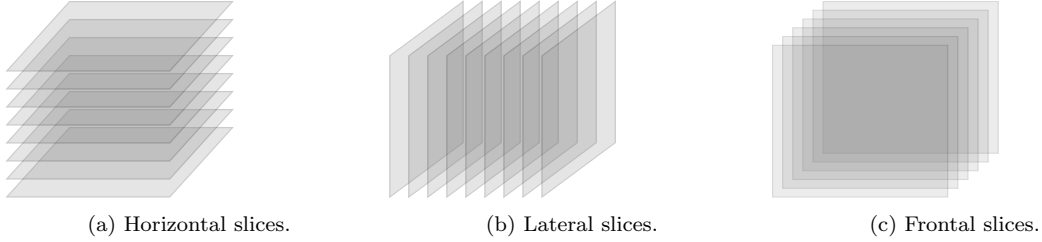


Fig. 7: Slices representations of the three-way tensor.

The order of tensor is referred to as the number of dimensions, also called ways or modes. One-mode tensor is a vector, second-order tensor is a matrix, and third-order tensor is a cuboid. In the case of matrix \mathbf{X} , a row and column can be denoted by $\mathbf{x}_{i\cdot}$ and $\mathbf{x}_{\cdot j}$, respectively. In the case of three-way tensor $\mathbf{x}_{ij\cdot}$, $\mathbf{x}_{i\cdot b}$, and $\mathbf{x}_{\cdot j b}$ represents the vector of the three different modes respectively. As we focus on *frontal slices*, the tensor can be represented by $\{\mathbf{X}^b, b = 1 \dots, v\}$ (Figure 7(c)). For convenience, in the following, we will denote the tensor entry $\mathbf{x}_{ij\cdot}$ by $\mathbf{x}_{ij} = (x_{ij}^1, \dots, x_{ij}^b, \dots, x_{ij}^v)$ (Figure 8); then $x_{i\cdot}^b = \sum_j x_{ij}^b$ and $x_{\cdot j}^b = \sum_i x_{ij}^b$. In this sequel, we aim to extract homogeneous sub-tensors from three-way data.

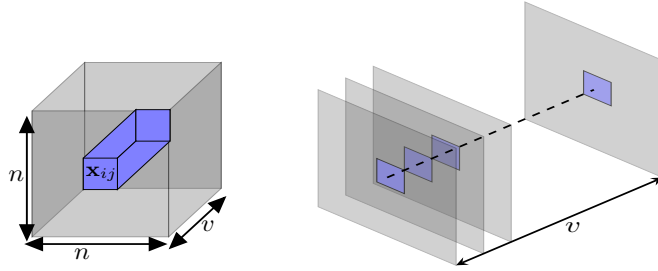


Fig. 8: The three-way tensor structure.

4.2 Definition of the proposed model

We extend SPLBM to Three-way tensor data leading to *Tensor SPLBM* (or TSPLBM). The proposed model seeks not only to discover homogeneous tube co-clusters (a three dimensional co-clusters) but also discover important blocks and ignore noisy ones. Thereby, TSPLBM allows to discover a diagonal co-clusters structure, which are tubes (through all slices) from the three-way tensor. It makes it more useful for sparse tensor with high sparsity close to 90%, as shown in the experiments. TSPLM

provides a better partitioning than the classical co-clustering algorithm applied on each slice of tensor separately or a consensus clustering used on these independent results.

Our proposal Tensor SPLBM considers 3D data matrix $\mathcal{X} = [\mathbf{x}_{ij}] \in \mathbb{R}^{n \times n \times v}$ where n is the number of nodes, and v the number of graphs (slices). Figure 1 presents a tensor data with v graphs. Assuming the independence per graph, the conditional Poisson pdf is given by

$$\prod_{i,j=1}^n \left(\prod_{k=1}^g \left\{ \prod_{b=1}^v \mathcal{P}(x_{ij}^b; x_i^b x_j^b \gamma_{k\ell}^b) \right\}^{z_{ik} w_{jk}} \prod_{k,\ell \neq k}^g \left\{ \prod_{b=1}^v \mathcal{P}(x_{ij}^b; x_i^b x_j^b \gamma^b) \right\}^{z_{ik} w_{j\ell}} \right).$$

As \mathcal{X} is symmetric per slice b , when $i = j$ we have $z_{ik} = w_{jk}$ and for $k = 1, \dots, g$ we have $\pi_k = \rho_k$. Then to optimize the lower bound of log-likelihood criterion noted $\mathcal{F}_C(\tilde{\mathbf{Z}}, \mathbf{\Omega})$ leads to optimize the following criterion (Eq. 3) (Appendix A for more details).

$$\frac{1}{2} \mathcal{F}_C(\tilde{\mathbf{Z}}, \mathbf{\Omega}) = \frac{1}{2} \mathcal{L}_C(\tilde{\mathbf{Z}}, \mathbf{\Omega}) + H(\tilde{\mathbf{Z}}) \quad (3)$$

where $H(\tilde{\mathbf{Z}}) = -\sum_{i,k} \tilde{z}_{ik} \log \tilde{z}_{ik}$ is the entropy, and $\mathcal{L}_C(\tilde{\mathbf{Z}}, \mathbf{\Omega})$ is the fuzzy complete log-likelihood function expressed by:

$$\mathcal{L}_C(\tilde{\mathbf{Z}}, \mathbf{\Omega}) = 2 \sum_{i,k} \tilde{z}_{ik} \log \pi_k + \sum_{i,j,k} \tilde{z}_{ik} \tilde{z}_{jk} \sum_{b=1}^v \log \mathcal{P}(x_{ij}^b; x_i^b x_j^b \gamma_{kk}^b) + \sum_{i,j,k,\ell \neq k} \tilde{z}_{ik} \tilde{z}_{j\ell} \sum_{b=1}^v \log \mathcal{P}(x_{ij}^b; x_i^b x_j^b \gamma^b).$$

After some algebraic calculations, we can simplify the criterion (up a constant) that takes the following form (for more details, please see Appendix B)

$$\sum_{i,k} \tilde{z}_{ik} \log \pi_k + \frac{1}{2} \sum_b \left(\sum_k \left[x_{kk}^b \log \left(\frac{\gamma_{kk}^b}{\gamma^b} \right) - x_k^b x_k^b (\gamma_{kk}^b - \gamma^b) \right] + N_b (\log(\gamma^b) - N_b^2 \gamma^b) \right) + H(\tilde{\mathbf{Z}}). \quad (4)$$

where $x_k^b = \sum_i \tilde{z}_{ik} x_i^b = \sum_j \tilde{z}_{jk} x_j^b = x_{k,k}^b$, $x_{kk}^b = \sum_{i,j} \tilde{z}_{ik} \tilde{z}_{jk} x_{ij}^b$, and $N_b = \sum_{i,j} x_{ij}^b$,

5 Variational Inference

To estimate the parameters of the model, we rely on the Variational EM algorithm (Govaert and Nadif, 2005), and we extend it to multiple graphs. In the sequel, the proposed algorithm is referred to as TSPLBM.

E-step. It consists in computing, for all i, j, k the posterior probabilities \tilde{z}_{ik} and \tilde{w}_{jk} given the estimated parameters $\mathbf{\Omega}$. As $\sum_k \tilde{z}_{ik} = \sum_k \tilde{z}_{jk} = 1$, using the corresponding Lagrangians, up to terms which are not function of \tilde{z}_{ik} , leads to

$$\log \tilde{z}_{ik}^{(t+1)} \propto \log \pi_k + \frac{1}{2} \left(\sum_{j,k} \tilde{z}_{jk}^{(t)} \sum_{b=1}^v \mathcal{P}_{kk}^{ijb} + \sum_{j \neq i, k \neq \ell} \tilde{z}_{j\ell}^{(t)} \sum_{b=1}^v \mathcal{P}_{k\ell}^{ijb} \right), \quad (5)$$

where $\mathcal{P}_{kk}^{ijb} = \log \mathcal{P}(x_{ij}^b; x_i^b x_j^b \gamma_{kk}^b)$ and with $k \neq \ell$, $\mathcal{P}_{k\ell}^{ijb} = \log \mathcal{P}(x_{ij}^b; x_i^b x_j^b \gamma^b)$. The update of $\tilde{z}_{ik}^{(t+1)}$ is described in Appendix C, and $\tilde{z}_{ik}^{(t)}$ represents the value of \tilde{z}_{ik} in the previous iteration (t).

M-step. Given the previously computed posterior probabilities $\tilde{\mathbf{Z}}$, the M-step consists in updating, $\forall k$, the parameters π_k , γ_{kk}^b and γ^b . The estimated parameters are defined as follows. First, taking into account the constraints $\sum_k \pi_k = 1$, it is easy to show that $\pi_k = \frac{\sum_i \tilde{z}_{ik}}{n}$. Secondly, it is easy to obtain for all b, k

$$\begin{aligned} \gamma_{kk}^b &= \frac{\sum_{i,j} \tilde{z}_{ik} \tilde{z}_{jk} x_{ij}^b}{\sum_i \tilde{z}_{ik} x_i^b \sum_j \tilde{z}_{jk} x_j^b} = \frac{x_{kk}^b}{[x_{k.}^b]^2} \text{ and,} \\ \gamma^b &= \frac{N_b - \sum_{i,j,k} \tilde{z}_{ik} \tilde{z}_{jk} x_{ij}^b}{N_b^2 - \sum_k \sum_i \tilde{z}_{ik} x_i^b \sum_j \tilde{z}_{jk} x_j^b} = \frac{N_b - \sum_k x_{kk}^b}{N_b^2 - \sum_k [x_{k.}^b]^2}. \end{aligned} \quad (6)$$

The TSPLBM algorithm (Algorithm 1) for multiple graphs (MG), alternates the two previously described steps Expectation-Maximization. At the convergence, a hard co-clustering is deduced from \tilde{z}_{ik} 's using the maximum a posteriori principle.

Algorithm 1: TSPLBM

Input: \mathcal{X} , g .

Initialization: $\mathbf{Z}^{(0)}$ randomly and compute $\Omega^{(0)}$, $t = 0$

repeat

E-Step: Compute $\tilde{z}_{ik}^{(t+1)}$

$$\tilde{z}_{ik}^{(t+1)} \propto \pi_k \exp\left(\frac{1}{2} \sum_j \tilde{z}_{jk}^{(t)} \sum_{b=1}^v x_{ij}^b \log\left(\frac{\gamma_{kk}^b}{\gamma^b}\right)\right)$$

M-Step: Update $\Omega^{(t+1)} = (\pi_k^{(t+1)}, (\gamma_{kk}^b)^{(t+1)}, (\gamma^b)^{(t+1)})$ given by

$$\pi_k = \frac{\sum_i \tilde{z}_{ik}^{(t+1)}}{n}, \gamma_{kk}^b = \frac{x_{kk}^b}{[x_{k.}^b]^2}, \text{ and } \gamma^b = \frac{N_b - \sum_k x_{kk}^b}{N_b^2 - \sum_k [x_{k.}^b]^2}$$

until the objective function value change is small or there is no change;

return \mathbf{Z} , Ω

6 Experiments

In our experiments, we aim to discuss three important questions about (i) The importance of considering multiple graphs simultaneously on clustering results through TSPLBM and comparison with baselines considering one graph each time. (ii) The second point shows how the proposed model can help with the interpretation of the obtained results. (iii) And finally, we made a parallel between the proposed approach and clustering ensemble, and we compare implicit consensus obtained by TSPLBM and the explicit consensus achieved by the clustering ensemble method.

6.1 Datasets and evaluation

We use four datasets with a different number of graphs (slices) and clusters. Table 1 shows the characteristics of datasets in terms of the type of instances (image or image+text), the number of graphs/slices (#Graphs), the number of instances (#Nodes), and the number of clusters (#Clusters). Hereafter, we give in detail, the description of each dataset..

Table 1: Characteristics of datasets.

Datasets	Type	#Graphs	#Nodes	#Clusters
DBLP1	Text	3	2223	3
DBLP3	Text	3	12550	10
Nus-Wide-8	Text+Images	6	2738	8
Amazon-products-10	Text+Images	7	9897	10

DBLP1 and DBLP3: The two datasets DBLP1 and DBLP3 are document datasets constructed from the global DBLP³ dataset. The clusters are represented by journals/conferences where the papers are published. We selected three journals ((and conferences) for DBLP1, namely Discrete Applied Mathematics, IEEE software, and SIGIR. For DBLP3, we selected ten journals (and conferences), which are ICC, IJCAI, SIGMOD, Discrete Applied Mathematics, Electr. Notes Theor. Comput. Sci., DAC, GECCO, ICIP, ICCV, and Journal of Systems and Software. We constructed three graphs. *Co-terms Title*, and *Co-terms Abstract*, are adjacency matrices representing the co-terms between documents on the title and abstract, respectively. The *Co-terms T* matrix is computed using $\mathcal{B}\mathcal{B}^\top$, where \mathcal{B} is a binarized documents-terms matrix, then $\forall i, \mathcal{T}_{ii} > 0$. We also have *Co-authors* graph denoting the number of joint authors for two documents.

Nus-Wide-8 dataset: It is a part of the Nus-Wide images dataset⁴ extracted using Flickr API. This dataset is composed of eight topics, namely Animals, Persons, Plants, Snow, Street, Temple, Town, and Wedding. We constructed six graphs — the *Co-tags* graph, which is an adjacency matrix of common tags between images. As described in the previous paragraph for *Co-terms* matrix, we used a binary matrix images-tags \mathcal{M} to compute *Co-tags* matrix \mathcal{H} by $\mathcal{M}\mathcal{M}^\top$. Other graphs are also created based on extracted features from images. The followed process to build graph similarity based on six extracted features form images including 64-D Color Histogram (CH), 144-D Color Correlogram (CORR), 73-D Edge direction histogram (EDH), 128-D Wavelet texture (WT), 225-D block-wise color moments (CW55). The computed similarity matrices are converted to adjacency matrices by putting one if the similarity is higher than ninety-seven percent quantile and zero otherwise.

Amazon-products-10 dataset: It is a part of the Amazon-products dataset⁵, composed of product images. We consider ten product categories, namely Beauty, Digital music, Home and kitchen, Office products, Cell phones, Sports and outdoors, Health and personal care, Clothing-Shoes-Jewelry, Patio-garden, and Baby. We constructed seven graphs. The three first one *Similarity LBP*, *Similarity Haralick* and *Similarity Gabor* are constructed based on Low Rank Representation (LRR) method (Liu et al., 2013a) for three different features namely 256-D Local Binary Patterns (LBP), 216-D Haralick features (Haralick et al., 1973) (considering distances $d = 1 \dots 9$, orientations $\theta = [0^\circ, 45^\circ, 90^\circ, 135^\circ]$) and 192-D Gabor features (Chengjun Liu and Wechsler, 2001) (considering scales $\sigma = 1 \dots 4$, orientations $\theta = [0^\circ, 45^\circ, 90^\circ, 135^\circ]$). The computed similarity matrices are converted to adjacency matrices by putting one if the similarity is higher than ninety-seven percent quantile and zero otherwise. *Co-terms Title* and *Co-terms Description* are adjacency matrices representing the co-terms between the title and description of products, respectively. Finally, *Co-viewed* and *Co-purchased* are adjacency matrices \mathcal{Y} , where $\mathcal{Y}_{ij} = 1$ means that these two products are viewed (respectively purchased) simultaneously when users make a query.

³ <https://aminer.org/citation>

⁴ <https://dl.acm.org/citation.cfm?id=1646452>

⁵ <http://jmcauley.ucsd.edu/data/amazon/links.html>

Figure 9 shows all graphs (slices) for the Amazon-products-10 dataset. The dataset is composed of seven graphs. We notice that each slice has different structures and different degrees of complexity. Our TSPLBM input is a tensor (Node \times Node \times Graph) for each dataset DBLP1, DBLP3, Nus-Wide-8, and Amazon-products-10 with different sparsity 0.96, 0.99, 0.83, and 0.98 respectively.

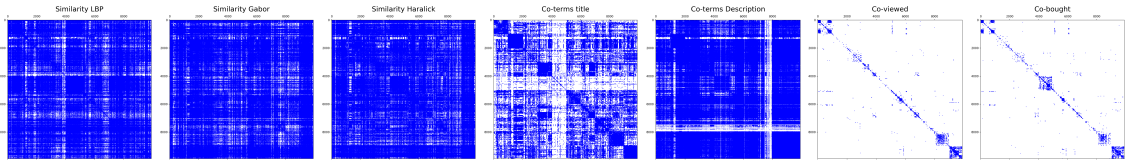


Fig. 9: Amazon-products-10 dataset.

What is the impact of considering multiple graphs on clustering results? We first compare TSPLBM applied on all graphs simultaneously with PSBM, PLBM, SPLBM used on each graph. The goal is to evaluate TSPLBM in terms of clustering with a comparison with the baselines. On the other hand, we aim to measure how the combination of different information through graphs, impacts, and improves results. Note that TSPLBM can be viewed as an ensemble method.

We perform 30 random initializations and compute Accuracy and Normalized Mutual Information (NMI) (Strehl and Ghosh, 2002) metrics by averaging all runs. The clustering accuracy noted (ACC) discovers the one-to-one relationship between two partitions and measures the extent to which each cluster contains data points from the corresponding class. However, NMI is based on Mutual Information (MI) and measures the amount of retrieved information considering our knowledge about the clusters and the obtained results by a clustering method while respecting the proportions of clusters.

In Figure 10, the performances of the four algorithms PSBM, PLBM, SPLBM, and TSPLBM on the four datasets, are reported. PSBM, PLBM, and SPLBM are applied on each slice (graph) separately. TSPLBM is applied to the tensor considering all graphs simultaneously. We notice that, in most cases, TSPLBM is better than other algorithms applied to each graph and allows us to achieve the best trade-off. TSPLBM includes all graphs and also the graphs with a very complex structure. DBLP3 obtains the lowest results due to the complex structure of dataset composed of 12K papers with very close or complementary topics on computer science. We observe that PLBM and SPLBM do a better job than PSBM for all datasets on the more informative slices. It is also worth noting that PLBM does good performances in terms of Accuracy on DBLP1 and in terms of NMI on DBLP3. TSPLBM performs a natural consensus when considering all slices and allows us to obtain a unique partition at the end with good clustering results.

How does the TSPLBM differ from multiview methods in terms of clustering performance?

The Multi-view clustering (MvC), Bickel and Scheffer (2004) aims to perform clustering from diverse sources or domains, where each object is described by several sets of features (or views). The MvC methods are used in several applications such as image clustering, where we can have different kinds of features. They allow to take into account the information arising of each view.

Because of the diversity of feature sets, each view can be converted to a symmetric instances \times instances similarity/dissimilarity matrix. This brings us back to a tensor representation of these views where each of them is a graph where the edges are continuous. Thereby, even though each view is not a count matrix, we compared TSPLBM—after binarisation—with two recent and effective algorithms S ω MV

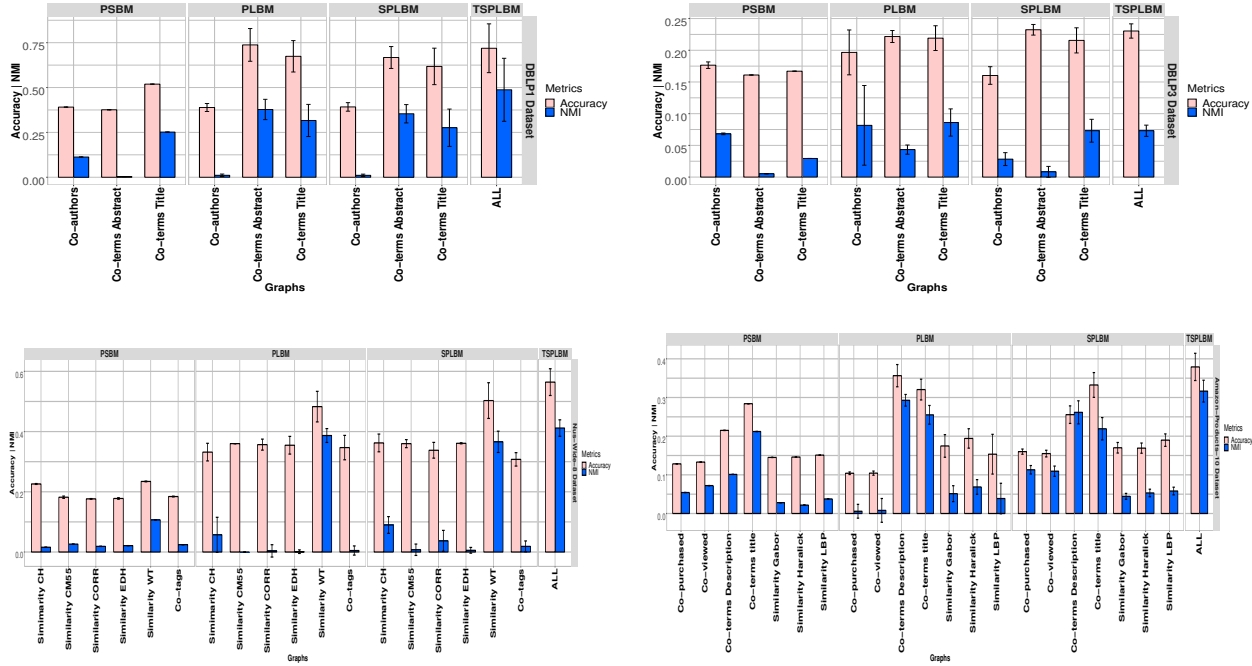


Fig. 10: Comparison in terms of Accuracy and NMI for all datasets with PSBM, PLBM, SPLBM and TSPLBM.

Nie et al. (2017) and **MultiNMF** Liu et al. (2013b). To evaluate the three algorithms, we selected six multi-view datasets UC-digits, 3sources, BBC, 100leaves, DBLP1, and Nus-Wide-8. These datasets are available at <https://github.com/KunyuLin/Multi-view-Datasets>.

We performed the same experimentation procedure as **TSPLBM** with 30 runs, and we compute the average of ACC, NMI, and Purity Sripada and Rao (2011). For the **MultiNMF**, we pricked up the results in terms of ACC and NMI that are available in these two papers Wang et al. (2020, 2015).

In Table 2 are reported the obtained results on the six multi-view datasets. Thereby **SwmV** does a better job than **MultiNMF**; it achieves good results on UC-digits and 100Leaves. However, **SwmV** could not give the clustering for DBLP1. On the other hand, **TSPLBM** achieves highly better results than **SwmV** on the four datasets.

Overall, from these experiments, even with binary edges, we observe that **TSPLBM** gives encouraging results compared with **SwmV** and **MultiNMF** applied on graphs with continuous edges.

Comparison between TSPLBM and tensor decomposition approaches Undoubtedly and for a long time, to deal with tensor data $\mathcal{X} \in \mathbb{R}^{n \times n \times v}$, the tensor decomposition methods are the most popular (Kolda and Bader, 2009). Even if they are not devoted to clustering, they allow to contribute to this task. Actually, these methods return a factor matrix $\in \mathbb{R}^{n \times r}$ (r is a given rank) for each mode that can be used for clustering. In the following, we focus on only one mode. Thus, we used a list of suitable algorithms for the clustering: **Kmeans++** (Arthur and Vassilvitskii, 2007), **Spectral clustering (SC)** (Ng et al., 2001), and the EM algorithm (Dempster et al., 1977) derived from *diagonal Gaussian Mixture Model (GMM)* available in the **Scikit-Learn** package. Thereby, we compared

Table 2: Mutiview Clustering performance comparison.

Datasets	MultiNMF ¹		SwMV ²			TSPLBM		
	ACC	NMI	ACC	NMI	Purity	ACC	NMI	Purity
UC-digits	0.88	0.80	0.94	0.91	0.95	0.74	0.80	0.76
3sources	0.48	0.46	0.35	0.10	0.36	0.66	0.54	0.66
BBC	0.48	0.33	0.33	0.05	0.33	0.66	0.66	0.66
100leaves	0.67	0.86	0.59	0.87	0.61	0.46	0.81	0.46
DBLP1	-	-	NA	NA	NA	0.83	0.57	0.85
Nus-Wide-8	-	-	0.28	0.004	0.28	0.56	0.41	0.56

¹ - symbol means that we could not retrieve the results for MultiNMF for these datasets.

² NA symbol means that the SwMV algorithm could not find clustering solution.

the sparse tensor co-clustering algorithm TSPLBM with PARAFAC (Harshman and Lundy, 1994) and Tucker decomposition (Tucker, 1966) on the six datasets presented in the previous section.

We use different ranks (10, 20 and 50). We performed 30 runs with random initialization. Then we computed ACC, NMI, and purity by averaging all runs. In figure 11 are reported the obtained

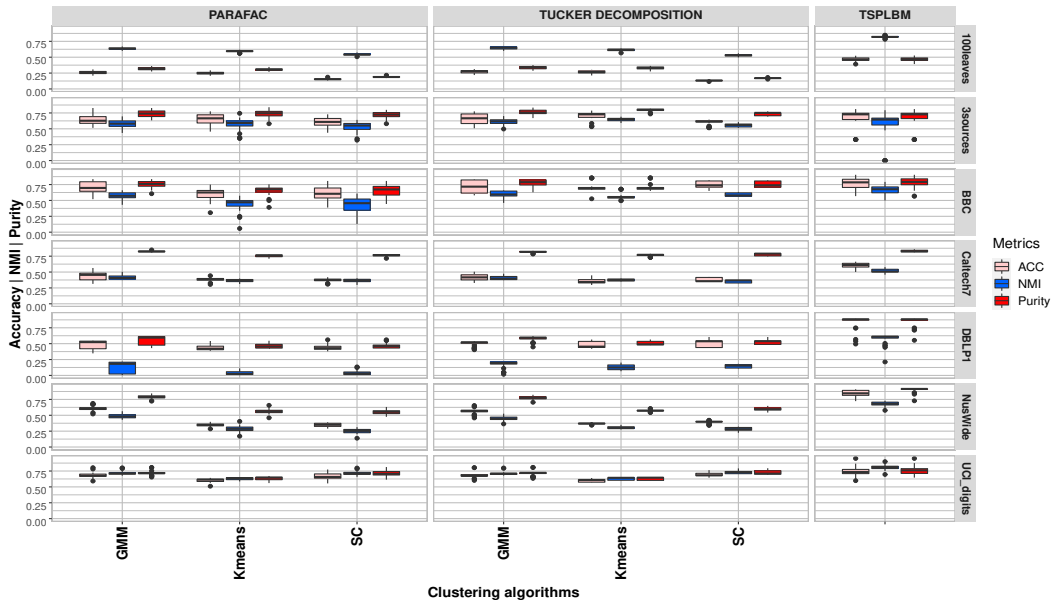


Fig. 11: Comparison between TSPLBM and tensor decomposition approaches based on clustering performances.

clustering results for the six datasets according to the different tensor-based algorithms (PARAFAC, Tucker decomposition, and TSPLBM) and the clustering algorithms applied on the obtained tensor decomposition. The results concern tensor decomposition approaches with rank number equal to 10 (The results for rank 20 and 50 are similar to those using rank equal to 10). We observe that in major cases for the six datasets the TSPLBM does a better job than PARAFAC and Tucker decomposition. For the 3sources and Caltech-7 datasets, PARAFAC and Tucker decomposition with GMM obtained close results in terms of Purity and Accuracy but TSPLBM achieves higher performances in terms of NMI.

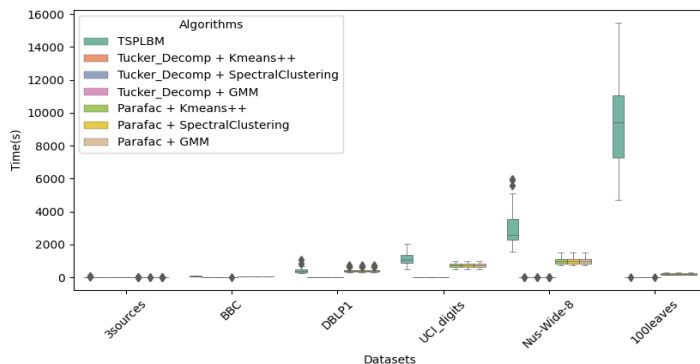


Fig. 12: Time complexity analysis.

To evaluate the computing time of TSPLBM comparing to tensor decomposition approaches, we represent in figure 12 the time execution in seconds of the compared methods for each dataset. We notice that for the four datasets 3sources, BBC, DBLP1, and UCI-digits, TSPLBM is close to all other approaches in terms of time execution. However, with Nus-wide-8 and 100Leaves, the time execution is more important, this is due to the dataset size and the number of clusters for Nus-wide-8 and 100Leaves. In figure 11, we observe however, that TSPLBM outperforms tensor decomposition approaches with approximately 25 points of ACC for these two datasets.

How can the proposed model help us in the interpretation of the obtained results? The objective of this part is to analyze the obtained topics and demonstrate how the proposed model can help and then improve the interpretation of the obtained clusters.

The second analysis that we made is dimensionality reduction of topics-tags matrix using the correspondence analysis method (CA) (Benzecri, 1973; Nenadic and Greenacre, 2007). The choice of CA is due to the connection between mutual information and chi-square, which is based in CA, see, e.g., (Govaert and Nadif, 2018). The matrix topic-tags $\mathbf{Z}^T \mathcal{M}$ is constructed from *image-tags* \mathcal{M} based on obtained topics (or partition) \mathbf{Z} obtained by TSPLBM. In Figure 13, are projected the tags and topics on the two first dimensions of CA including the top tags in terms of contribution⁶ on the CA results.

We can notice that there are some close topics and other very different one. For instance, topic 3 about weddings is opposed to topics 8 and 6 about *snow* and *temple* considering the first and the second dimension respectively. On the other hand, we can see that topics 1 and 2 about plants and animals are close.

Figure 14 presents the tags whose contribution is important. We show the frequencies of each term for each topic. For topics 2 and 5 (pink and purple color respectively), we can see that the four top tags are *Nature*, *Green*, *Macro*, and *Flower* related to Plants topic and *Street*, *City*, *Night* and *Architect* related to Town topic.

Based on the *Co-tags* graph and the obtained topics, we construct a graph of image clusters linked by edges representing the intensity of joint tags between all topics, this can be computed by $\mathbf{Z}^T \mathcal{H} \mathbf{Z}$ where \mathbf{Z} is obtained by TSPLBM, and \mathcal{H} is the co-tags matrix. We can notice that there are some topics with a strong relationship like *plants-snow* and *town-persons*. On the other hand, some topics with a weak link like *animals-town* and *animals-temple*. This representation highlights that there are

⁶ With CA each tag contributes to the inertia of each axis. The contribution of a tag to axis α is expressed as a percent of the inertia for axis α .

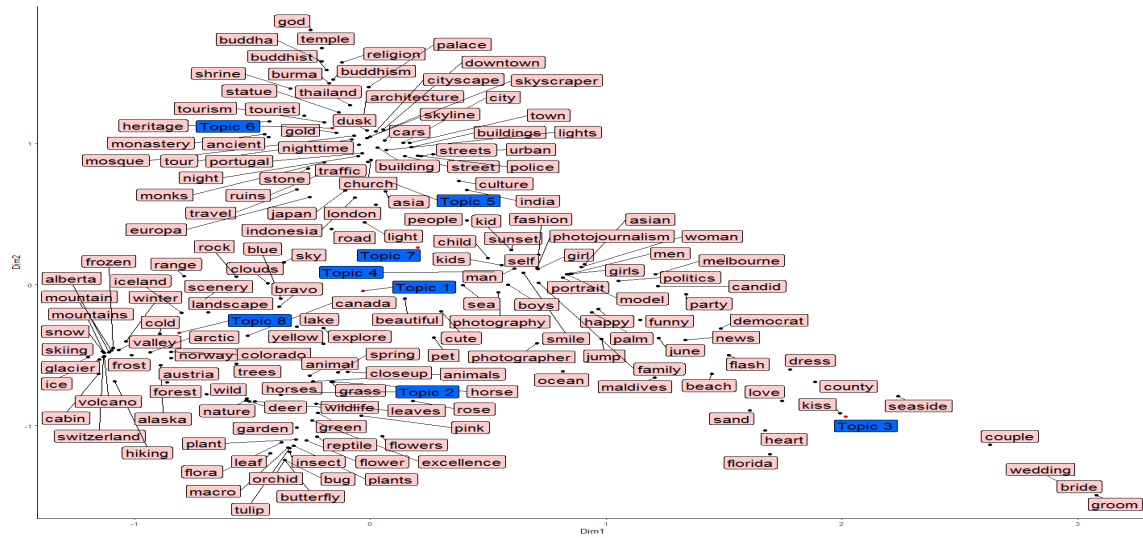


Fig. 13: CA applied on topic-tags matrix.



Fig. 14: Frequency matrix of subject tags whose contribution is important.

some tags used with confused meaning. In this context, it is possible to use tensor models for tags completion and tags correction (Tang et al., 2017; Veit et al., 2017).

6.2 Implicit consensus vs. explicit consensus

In the first part of our experiments, we have observed that TSPLBM applied on all slices simultaneously is, in most cases, better than other algorithms. As we are in an unsupervised context, we have found it helpful to run the calculation with several different random initial conditions and take the best result in terms of maximum log-likelihood, overall runs.

Figure 15 shows the 30 performed runs sorted according to Normalized log-likelihood (NL), which is the objective function of TSPLBM. We also draw the ACC and NMI curve according to the 30 runs. We observe that for DBLP1, the best runs leading to maximal NL are the best runs in terms of clustering (ACC and NMI). However, this observation is not noticed in all datasets; for instance, some best runs can achieve less good results in terms of ACC and NMI. This problem is recurrent with all unsupervised methods where the best runs in terms of the objective function are not necessarily the best ones in terms of clustering. On the other hand, we may see the proposed model as an implicit consensus model for graphs clustering, and it is tempting to compare the proposed model to ensemble-based clustering methods.

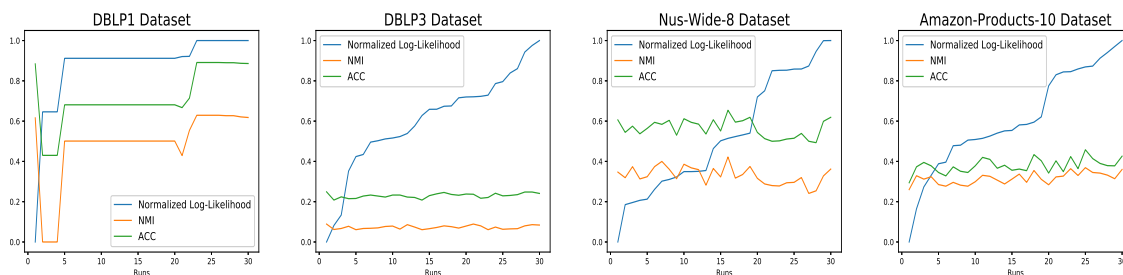


Fig. 15: Normalized Log-likelihood *vs* NMI and ACC for all runs.

The first works about consensus or ensemble classification have emerged in the context of supervised learning; see for instance (Maclin and Opitz, 1997; Schapire, 2003; Dietterich, 2000). However, only the majority voting type algorithms work on the model output level, and the most well-known classification ensembles approaches are based on different variants of voting (Bauer and Kohavi, 1999; Cramer et al., 2008; Gao et al., 2009). This approach has been extended to unsupervised learning (Strehl and Ghosh, 2002; Vega-Pons and Ruiz-Shulcloper, 2011). A clustering ensemble, also known as a consensus clustering or clustering aggregation, is defined in the same manner as for classification (Hanczar and Nadif, 2012; Alqurashi and Wang, 2019; Yu et al., 2019). It consists in combining multiple clustering models (partitions) into a single consolidated partition that we refer to as *explicit* consensus clustering. In other words, from r partitions $\{\mathbf{Z}_1, \mathbf{Z}_2, \mathbf{Z}_3, \dots, \mathbf{Z}_r\}$, a consensus clustering leads to a unique partition \mathbf{Z}^* . Based on consensus functions, many approaches exist; see for instance (Strehl and Ghosh, 2002; Hanczar and Nadif, 2012; Affeldt et al., 2020a,b).

In (Strehl and Ghosh, 2002), the authors introduced three ensemble clustering methods that can produce a consensus partition. All of them consider the consensus problem on a hypergraph representation of the set of partitions. More specifically, each partition is a binary classification matrix (with objects in rows and clusters in columns) where the concatenation of all the set defines the hypergraph. Figure 16 presents this matrix and different steps to construct a combination of these different graphs of clusters, emerged from different partitions, to obtain a unique graph. To this end, we rely on the three hypergraph clustering-based approaches proposed by Strehl and Ghosh (2002), namely *CSPA* (Cluster-based Similarity Partitioning Algorithm), *HGPA* (HyperGraph Partitioning Algorithm), and *MCLA* (Meta-CLustering Algorithm). To improve clustering results of TSPLBM we will adopt the ensemble approach. We explore in the next part, how *implicit* consensus clustering through TSPLBM behaves compared to *explicit* consensus through cluster ensembles of multiple graphs. In Figure 17, we report the proposed approach to compare TSPLBM with the clustering ensemble methods proposed by Strehl

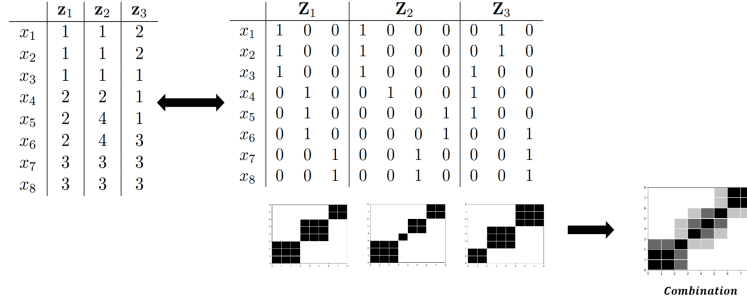


Fig. 16: Process of the transition from clustering to consensus clustering.

and Ghosh (2002). To do this, we used the implementation of python package `Cluster Ensembles`⁷. It relies on `CSPA`, `HGPA`, and `MCLA` and returns the best results in terms of the mean of NMI between the obtained consensus clustering Z^* and the different clustering solutions $\{Z_1, Z_2, Z_3, \dots, Z_r\}$. Thereby, with `TSPBLM`, we select the top ten runs maximizing log-likelihood then we carry out the consensus by using the cluster-ensembles methods. With `SPLBM`, `PLBM`, and `PSBM`, we consider two steps. The first step is the same as that used with `TSPBLM` to select the top ten runs and apply the cluster-ensembles methods. The second one consists in applying another clustering consensus between graphs to obtain a unique partition. Note that the slice consensus is implicitly provided by the `TSPBLM` algorithm.

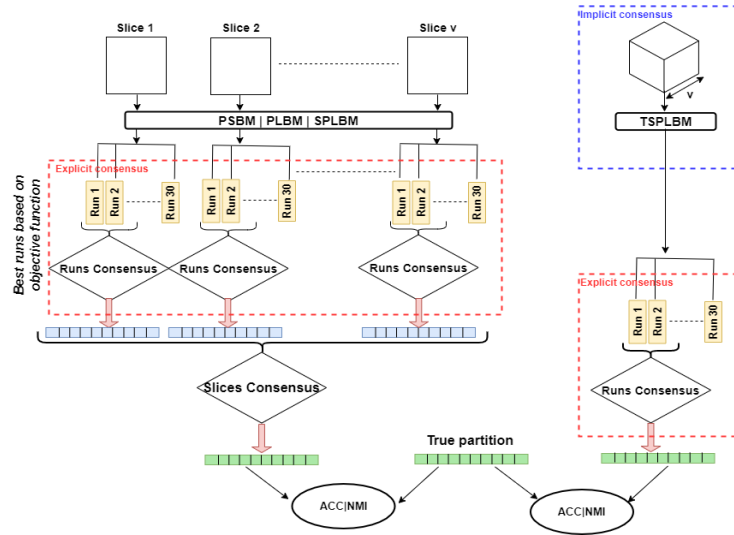


Fig. 17: Ensemble methods with `PSBM`, `PLBM`, `SPSEBM` and `TSPBLM`. Description of the assessment process of all algorithms in terms of ACC and NMI.

In Figure 18 are reported the obtained results in terms of NMI using the comparison approach described above. We can notice that `TSPBLM` achieves the highest NMI for all datasets. `SPLBM` does a

⁷ https://pypi.org/project/Cluster_Ensembles/

better or similar job than PLBM on three datasets, while PSBM obtains the lowest NMI measures on all datasets. These results can be explained by the fact that the implicit consensus achieved by TSPLBM is optimized within the objective function of the algorithm, unlike the explicit consensus, where the partitions are obtained separately.

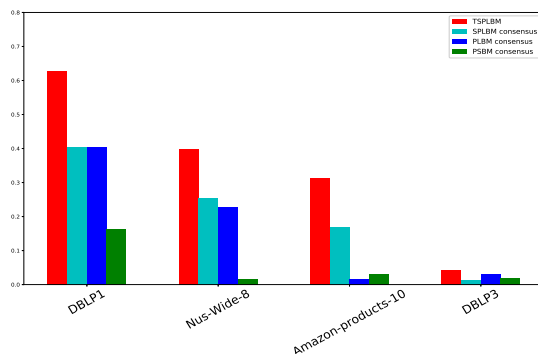


Fig. 18: Consensus clustering based NMI comparison.

7 Conclusion

It is well known that the traditional Poisson SBM fails to detect relevant clusters of edges, this requires a degree-corrected SBM (DC-SBM). Drawing on this, we first established some connections between Poisson SBM and the corrected version DC-SBM with Poisson LBM commonly used for the co-clustering of contingency tables. We justified the extension of the latter to deal with multiple graphs clustering. To take into account the sparsity of the tensor, we modified the parametrization of the model and proposed a Tensor SPLBM (TSPLBM). We derived, thereby, an EM-like learning algorithm called TSPLBM capable of performing clustering from a tensor data. On real datasets of text and image graphs, we have shown that TSPLBM, is better than the cited baselines algorithms in terms of clustering.

On the other hand, we can note that the proposed clustering algorithm TSPLBM can be seen as an implicit consensus clustering between multiple graphs. To reinforce our idea that TSPLBM can be used in this sense, a comparative study with explicit consensus through ensemble clustering methods was realized. Experiments on several real graphs datasets highlight the effectiveness of TSPLBM. Thereby, this work gives an extra dimension to LBM as an ensemble method.

Our approach has made it possible to propose a like-EM learning algorithm. It is possible to develop a like-Classification EM version. To do this, all that is needed is to insert a classification step between E and M steps. This could lead to propose an extension of DC-SBM for multiple graphs. In this paper, the number of clusters has been assumed to be known, it would be interesting to propose an extension of some criteria, such as ICL (Integrated Completed Likelihood) criterion, already used with SBM (Daudin et al., 2008).

A Appendix: Proof of Equation 3

The marginal density function $f(\mathbf{X}; \Omega)$ of TSPLBM can be written as:

$$f(\mathbf{X}; \Omega) = \sum_{(\mathbf{z}, \mathbf{w}) \in \mathcal{Z} \times \mathcal{W}} \prod_{i,k} \pi_k^{z_{ik}} \prod_{j,k} \rho_k^{w_{jk}} \prod_{i,j=1}^n \prod_{k=1}^g \left\{ \prod_{b=1}^v \mathcal{P}(x_{ij}^b; x_i^b, x_j^b, \gamma_{kk}^b) \right\}^{z_{ik} w_{jk}} \prod_{k, \ell \neq k}^g \left\{ \prod_{b=1}^v \mathcal{P}(x_{ij}^b; x_i^b, x_j^b, \gamma^b) \right\}^{z_{ik} w_{j\ell}}.$$

Thus, the complete-data log-likelihood function is given by:

$$\mathcal{L}_C(\mathbf{Z}, \mathbf{W}, \Omega) = \sum_{i,k} z_{ik} \log \pi_k + \sum_{j,k} w_{jk} \log \rho_k + \sum_k \mathcal{L}_C^k$$

where

$$\mathcal{L}_C^k = \sum_{i,j} z_{ik} w_{jk} \left\{ \sum_{b=1}^v \mathcal{P}(x_{ij}^b; x_i^b, x_j^b, \gamma_{kk}^b) \right\} + \sum_{i,j, \ell \neq k} z_{ik} w_{j\ell} \left\{ \sum_{b=1}^v \mathcal{P}(x_{ij}^b; x_i^b, x_j^b, \gamma^b) \right\}.$$

Hence, the aim is to maximize the following lower bound of the log-likelihood criterion:

$$\mathcal{F}_C(\tilde{\mathbf{Z}}, \tilde{\mathbf{W}}, \Omega) = \mathcal{L}_C(\tilde{\mathbf{Z}}, \tilde{\mathbf{W}}, \Omega) + H(\tilde{\mathbf{Z}}) + H(\tilde{\mathbf{W}})$$

where $\mathcal{L}_C(\tilde{\mathbf{Z}}, \tilde{\mathbf{W}}, \Omega)$ is the fuzzy complete-data log-likelihood function. As \mathcal{X} is symmetric per slice b , when $i = j$ we have $z_{ik} = w_{jk}$ and for $k = 1, \dots, g$ we have $\pi_k = \rho_k$ and $H(\tilde{\mathbf{Z}}) = H(\tilde{\mathbf{W}})$. The $\mathcal{F}_C(\tilde{\mathbf{Z}}, \Omega)$ takes the following form:

$$\mathcal{F}_C(\tilde{\mathbf{Z}}, \Omega) = \mathcal{L}_C(\tilde{\mathbf{Z}}, \Omega) + 2H(\tilde{\mathbf{Z}}) \quad \text{with} \quad \mathcal{L}_C(\tilde{\mathbf{Z}}, \Omega) = 2 \sum_{i,k} \tilde{z}_{ik} \log \pi_k + \sum_k \mathcal{L}_C^k.$$

Then, we can simplify the model by optimizing $\frac{1}{2} \mathcal{F}_C(\tilde{\mathbf{Z}}, \Omega)$ leading to optimizing $\frac{1}{2} \mathcal{L}_C(\tilde{\mathbf{Z}}, \Omega) + H(\tilde{\mathbf{Z}})$.

B Appendix: Proof of Equation 4

The simplified optimization criterion can be written as:

$$\begin{aligned} & \sum_{i,k} \tilde{z}_{ik} \log \pi_k + \frac{1}{2} \sum_{i,j,k} \tilde{z}_{ik} \tilde{z}_{jk} \sum_{b=1}^v \log \mathcal{P}(x_{ij}^b; x_i^b, x_j^b, \gamma_{kk}^b) + \frac{1}{2} \sum_{i,j,k, \ell \neq k} \tilde{z}_{ik} \tilde{z}_{j\ell} \sum_{b=1}^v \log \mathcal{P}(x_{ij}^b; x_i^b, x_j^b, \gamma^b) + H(\tilde{\mathbf{Z}}) \\ &= \sum_{i,k} \tilde{z}_{ik} \log \pi_k + \frac{1}{2} \left[\sum_{i,j,k} \tilde{z}_{ik} \tilde{z}_{jk} \sum_b \log \left(\frac{e^{-x_i^b} x_j^b \gamma_{kk}^b (x_i^b x_j^b \gamma_{kk}^b)^{x_{ij}^b}}{x_{ij}^b!} \right) + \sum_{i,j,k, \ell \neq k} \tilde{z}_{ik} \tilde{z}_{j\ell} \sum_b \left(\frac{e^{-x_i^b} x_j^b \gamma^b (x_i^b x_j^b \gamma^b)^{x_{ij}^b}}{x_{ij}^b!} \right) \right] \\ &+ H(\tilde{\mathbf{Z}}) \\ &= \sum_{i,k} \tilde{z}_{ik} \log \pi_k + \frac{1}{2} \left[\sum_{i,j,k} \tilde{z}_{ik} \tilde{z}_{jk} \sum_b \left(-x_i^b x_j^b \gamma_{kk}^b + x_{ij}^b \log \gamma_{kk}^b \right) + \sum_{i,j,k, \ell \neq k} \tilde{z}_{ik} \tilde{z}_{j\ell} \sum_b \left(-x_i^b x_j^b \gamma^b + x_{ij}^b \log \gamma^b \right) \right] \\ &+ \sum_{i,j,b} x_{ij}^b \log(x_i^b x_j^b) - \log(x_{ij}^b!) + H(\tilde{\mathbf{Z}}) \end{aligned}$$

Note that the term $\sum_{i,j,b} x_{ij}^b \log(x_i^b x_j^b) - \log(x_{ij}^b!)$ is a scalar which does not depend on \mathbf{z} , \mathbf{w} , and Ω and therefore can be ignored for optimization purpose. To keep formulas uncluttered we therefore discard this term in the subsequent development. Thus, we obtain:

$$\sum_{i,k} \tilde{z}_{ik} \log \pi_k + \frac{1}{2} \sum_b \sum_k \left(x_{kk}^b \log(\gamma_{kk}^b) - x_k^b x_k^b \gamma_{kk}^b \right) + \frac{1}{2} \sum_b \left(\left(N_b - \sum_k x_{kk}^b \right) \log(\gamma^b) - \left(N_b^2 - \sum_k x_k^b x_k^b \right) \gamma^b \right) + H(\tilde{\mathbf{Z}})$$

where $N^b = \sum_{i,j} x_{ij}^b$ xxxxxxxxxx

$$\sum_{i,k} \tilde{z}_{ik} \log \pi_k + \frac{1}{2} \sum_b \left(\sum_k \left[x_{kk}^b \log \left(\frac{\gamma_{kk}^b}{\gamma^b} \right) - x_k^b x_k^b (\gamma_{kk}^b - \gamma^b) \right] + N_b (\log(\gamma^b) - N_b \gamma^b) \right) + H(\tilde{\mathbf{Z}}).$$

C Appendix: Update $\tilde{z}_{ik} \forall i, k$

To obtain the expression of \tilde{z}_{ik} , we maximize (3) with respect to \tilde{z}_{ik} , subject to the constraint $\sum_k \tilde{z}_{ik} = 1$. The corresponding Lagrangian, up to terms which are not a function of \tilde{z}_{ik} , is given by :

$$L(\tilde{\mathbf{z}}, \beta) = \sum_{i,k} \tilde{z}_{ik} \log \pi_k + \frac{1}{2} \sum_{i,j,k} \tilde{z}_{ik} \tilde{z}_{jk} \left(\sum_{b=1}^v \mathcal{P}_{kk}^{ijb} \right) + \frac{1}{2} \sum_{i \neq j, k \neq \ell} \tilde{z}_{ik} \tilde{z}_{j\ell} \left(\sum_{b=1}^v \mathcal{P}_{k\ell}^{ijb} \right) - \sum_{i,k} \tilde{z}_{ik} \log(\tilde{z}_{ik}) + \beta (1 - \sum_k \tilde{z}_{ik}).$$

Taking derivatives with respect to \tilde{z}_{ik} , we obtain:

$$\frac{\partial L(\tilde{\mathbf{z}}, \beta)}{\partial \tilde{z}_{ik}} = \log \pi_k + \frac{1}{2} \sum_{j,k} \tilde{z}_{jk} \left(\sum_{b=1}^v \mathcal{P}_{kk}^{ijb} \right) + \frac{1}{2} \sum_{j \neq i, k \neq \ell} \tilde{z}_{j\ell} \left(\sum_{b=1}^v \mathcal{P}_{k\ell}^{ijb} \right) - \log \tilde{z}_{ik} - 1 - \beta.$$

Setting this derivative to zero yields:

$$\tilde{z}_{ik} = \frac{\pi_k \exp \frac{1}{2} \left(\sum_{j,k} \tilde{z}_{jk} \sum_{b=1}^v \mathcal{P}_{kk}^{ijb} + \sum_{j \neq i, k \neq \ell} \tilde{z}_{j\ell} \sum_{b=1}^v \mathcal{P}_{k\ell}^{ijb} \right)}{\exp(\beta + 1)}.$$

Summing both sides over all k' yields $\exp(\beta+1) = \sum_{k'} \pi_{k'} \exp \frac{1}{2} \left(\sum_{j,k'} \tilde{z}_{jk'} \sum_{b=1}^v \mathcal{P}_{k'k'}^{ijb} + \sum_{j \neq i, k' \neq \ell} \tilde{z}_{j\ell} \sum_{b=1}^v \mathcal{P}_{k'\ell}^{ijb} \right)$. Plugging $\exp(\beta + 1)$ in \tilde{z}_{ik} leads to:

$$\tilde{z}_{ik} \propto \pi_k \exp \frac{1}{2} \left(\sum_{j,k} \tilde{z}_{jk} \sum_{b=1}^v \mathcal{P}_{kk}^{ijb} + \sum_{j \neq i, k \neq \ell} \tilde{z}_{j\ell} \sum_{b=1}^v \mathcal{P}_{k\ell}^{ijb} \right)$$

equivalent to

$$\log \tilde{z}_{ik} \propto \log \pi_k + \frac{1}{2} \left(\sum_{j,k} \tilde{z}_{jk} \sum_{b=1}^v \mathcal{P}_{kk}^{ijb} + \sum_{j \neq i, k \neq \ell} \tilde{z}_{j\ell} \sum_{b=1}^v \mathcal{P}_{k\ell}^{ijb} \right).$$

Now, based on simplification obtained in equation 4, the expression $\frac{1}{2} \left(\sum_{j,k} \tilde{z}_{jk} \sum_{b=1}^v \mathcal{P}_{kk}^{ijb} + \sum_{j \neq i, k \neq \ell} \tilde{z}_{j\ell} \sum_{b=1}^v \mathcal{P}_{k\ell}^{ijb} \right)$ can be written as:

$$\begin{aligned} & \frac{1}{2} \sum_b \left(\sum_k \left[x_{kk}^b \log \left(\frac{\gamma_{kk}^b}{\gamma^b} \right) - x_{k.}^b x_{.k}^b (\gamma_{kk}^b - \gamma^b) \right] + N_b (\log(\gamma^b) - N_b^2 \gamma^b) \right) \\ & = \frac{1}{2} \sum_b \left(\sum_k x_{kk}^b \log \left(\frac{\gamma_{kk}^b}{\gamma^b} \right) - [x_{k.}^b]^2 \gamma_{kk}^b - \gamma^b (N_b^2 - [x_{k.}^b]^2) + N_b (\log(\gamma^b)) \right) \end{aligned}$$

Thus, plugging the estimation of γ_{kk}^b 's and γ^b (equation 6) yields to :

$$\begin{aligned} & \frac{1}{2} \sum_b \left(\sum_k x_{kk}^b \log \left(\frac{\gamma_{kk}^b}{\gamma^b} \right) - [x_{k.}^b]^2 \frac{x_{kk}^b}{[x_{k.}^b]^2} - \frac{N_b - \sum_k x_{kk}^b}{N_b^2 - \sum_k [x_{k.}^b]^2} (N_b^2 - [x_{k.}^b]^2) + N_b (\log(\gamma^b)) \right) \\ & = \frac{1}{2} \sum_b \left(\sum_k x_{kk}^b \log \left(\frac{\gamma_{kk}^b}{\gamma^b} \right) + N_b (\log(\gamma^b) - 1) \right) \end{aligned}$$

The term $N_b (\log(\gamma^b) - 1)$ does not depend on \tilde{z}_{ik} we can simplify the expression to:

$$\frac{1}{2} \sum_b \left(\sum_k x_{kk}^b \log \left(\frac{\gamma_{kk}^b}{\gamma^b} \right) \right)$$

Finally, considering a particular k , we can re-write the equation C as:

$$\tilde{z}_{ik}^{(t+1)} \propto \pi_k \exp \left(\frac{1}{2} \sum_j \tilde{z}_{jk}^{(t)} \sum_{b=1}^v x_{ij}^b \log \left(\frac{\gamma_{kk}^b}{\gamma^b} \right) \right)$$

Funding Our work is funded by the German Federal Ministry for Economic Affairs and Energy (BMWi) under grant agreement number 01MK20008F (Service-Meister).

References

- Affeldt S, Labiod L, Nadif M (2020a) Ensemble block co-clustering: A unified framework for text data. In: Proceedings of the 29th ACM International Conference on Information & Knowledge Management, pp 5–14
- Affeldt S, Labiod L, Nadif M (2020b) Spectral clustering via ensemble deep autoencoder learning (SC-EDAE). *Pattern Recognition* 108:107522
- Ailem M, Role F, Nadif M (2017a) Model-based co-clustering for the effective handling of sparse data. *Pattern Recognition* 72:108–122
- Ailem M, Role F, Nadif M (2017b) Sparse poisson latent block model for document clustering. *IEEE Transactions on Knowledge and Data Engineering* 29(7):1563–1576
- Alqurashi T, Wang W (2019) Clustering ensemble method. *International Journal of Machine Learning and Cybernetics* 10(6):1227–1246
- Arthur D, Vassilvitskii S (2007) K-means++: The advantages of careful seeding. In: Proceedings of the Eighteenth Annual ACM-SIAM Symposium on Discrete Algorithms, Society for Industrial and Applied Mathematics, USA, SODA '07, p 1027–1035
- Banerjee A, Basu S, Merugu S (2007) Multi-way clustering on relation graphs. In: SIAM international conference on data mining, pp 145–156
- Bauer E, Kohavi R (1999) An empirical comparison of voting classification algorithms: Bagging, boosting, and variants. *Machine learning* 36(1-2):105–139
- Benzecri JP (1973) L'analyse des données, tome 2 : l'analyse des correspondances. Dunod, Paris
- Bickel S, Scheffer T (2004) Multi-view clustering. In: ICDM, Citeseer, vol 4, pp 19–26
- Celeux G, Govaert G (1992) A classification EM algorithm for clustering and two stochastic versions. *Computational Statistics and Data Analysis* 14(3):315–332
- Chen C, Ng MK, Zhang S (2017) Block spectral clustering methods for multiple graphs. *Numerical Linear Algebra with Applications* 24(1):e2075
- Chengjun Liu, Wechsler H (2001) A gabor feature classifier for face recognition. In: Proceedings Eighth IEEE International Conference on Computer Vision. ICCV 2001, vol 2, pp 270–275
- Crammer K, Kearns M, Wortman J (2008) Learning from multiple sources. *Journal of Machine Learning Research* 9(Aug):1757–1774
- Daudin JJ, Picard F, Robin S (2008) A mixture model for random graphs. *Statistics and computing* 18(2):173–183
- Dempster AP, Laird NM, Rubin DB (1977) Maximum likelihood from incomplete data via the EM algorithm. *Journal of the Royal Statistical Society: Series B* 39:1–38
- Dhillon IS, Mallela S, Modha DS (2003) Information-theoretic co-clustering. In: Proceedings of the Ninth ACM SIGKDD, pp 89–98
- Dietterich TG (2000) Ensemble methods in machine learning. In: International workshop on multiple classifier systems, Springer, pp 1–15
- Frankel T (2012) *The Geometry of Physics: An Introduction*. Cambridge University Press
- Gao J, Liang F, Fan W, Sun Y, Han J (2009) Graph-based consensus maximization among multiple supervised and unsupervised models. In: *Advances in Neural Information Processing Systems*, pp 585–593
- Govaert G, Nadif M (2003) Clustering with block mixture models. *Pattern Recognition* 36:463–473
- Govaert G, Nadif M (2005) An EM algorithm for the block mixture model. *IEEE Transactions on Pattern Analysis and machine intelligence* 27(4):643–647
- Govaert G, Nadif M (2013) *Co-clustering: models, algorithms and applications*. John Wiley & Sons
- Govaert G, Nadif M (2018) Mutual information, phi-squared and model-based co-clustering for contingency tables. *Advances in Data Analysis and Classification* 12(3):455–488
- Hanczar B, Nadif M (2012) Ensemble methods for biclustering tasks. *Pattern Recognition* 45(11):3938–3949
- Haralick R, Shanmugam K, Dinstein I (1973) Textural features for image classification. *IEEE Transactions on Systems, Man, and Cybernetics* 3(6):610–621
- Harshman RA, Lundy ME (1994) Parafac : parallel factor analysis. *Computational statistics and data analysis* 18:39–72
- Janson S (1987) Poisson convergence and poisson processes with applications to random graphs. *Stochastic Processes and their Applications* 26:1 – 30
- Karrer B, Newman ME (2011) Stochastic blockmodels and community structure in networks. *Physical review E* 83(1):016107
- Kiers HA (2000) Towards a standardized notation and terminology in multiway analysis. *Journal of Chemometrics* 14:105–122

- Kolda TG, Bader BW (2009) Tensor decompositions and applications. *Journal of mathematical psychology* 51(3):455–500
- Liu G, Lin Z, Yan S, Sun J, Yu Y, Ma Y (2013a) Robust recovery of subspace structures by low-rank representation. *IEEE transactions on pattern analysis and machine intelligence* 35(1):171–184
- Liu J, Wang C, Gao J, Han J (2013b) Multi-view clustering via joint nonnegative matrix factorization. In: *Proceedings of the 2013 SIAM International Conference on Data Mining*, SIAM, pp 252–260
- Maclin R, Opitz D (1997) An empirical evaluation of bagging and boosting. *AAAI/IAAI 1997*:546–551
- McLachlan GJ, Peel D (2000) *Finite Mixture Models*. Wiley, New York
- Nadif M, Govaert G (2005) Block clustering of contingency table and mixture model. In: *International Symposium on Intelligent Data Analysis*, Springer, pp 249–259
- Neal RM, Hinton GE (1998) A view of the em algorithm that justifies incremental, sparse, and other variants. In: *Learning in graphical models*, Springer, pp 355–368
- Nenadic O, Greenacre M (2007) Correspondence analysis in R, with two-and three-dimensional graphics: The CA package. *Journal of statistical software* 20(3)
- Ng A, Jordan M, Weiss Y (2001) On spectral clustering: Analysis and an algorithm. *Advances in neural information processing systems* 14:849–856
- Nie F, Li J, Li X, et al. (2017) Self-weighted multiview clustering with multiple graphs. In: *IJCAI*, pp 2564–2570
- Nowicki K, Snijders TAB (2001) Estimation and prediction for stochastic blockstructures. *Journal of the American statistical association* 96(455):1077–1087
- Schapire RE (2003) The boosting approach to machine learning: An overview. In: *Nonlinear estimation and classification*, Springer, pp 149–171
- Shan H, Banerjee A (2008) Bayesian co-clustering. In: *2008 Eighth IEEE International Conference on Data Mining*, IEEE, pp 530–539
- Sripada SC, Rao MS (2011) Comparison of purity and entropy of k-means clustering and fuzzy c means clustering. *Indian journal of computer science and engineering* 2(3):343–346
- Strehl A, Ghosh J (2002) Cluster ensembles - a knowledge reuse framework for combining multiple partitions. *Journal of Machine Learning Research* 3:583–617
- Tang J, Shu X, Qi G, Li Z, Wang M, Yan S, Jain R (2017) Tri-clustered tensor completion for social-aware image tag refinement. *IEEE Transactions on Pattern Analysis and Machine Intelligence* 39(8):1662–1674
- Tang W, Lu Z, Dhillon IS (2009) Clustering with multiple graphs. In: *2009 Ninth IEEE International Conference on Data Mining*, IEEE, pp 1016–1021
- Tucker LR (1966) Some mathematical notes on three-mode factor analysis. *Psychometrika* 31(3):279–311
- Vega-Pons S, Ruiz-Shulcloper J (2011) A survey of clustering ensemble algorithms. *International Journal of Pattern Recognition and Artificial Intelligence* 25(03):337–372
- Veit A, Nickel M, Belongie S, Maaten L (2017) Separating self-expression and visual content in hashtag supervision. In: *2018 IEEE/CVF Conference on Computer Vision and Pattern Recognition (CVPR)*
- Wang H, Yang Y, Liu B (2020) Gmc: Graph-based multi-view clustering. *IEEE Transactions on Knowledge and Data Engineering* 32(6):1116–1129
- Wang Z, Kong X, Fu H, Li M, Zhang Y (2015) Feature extraction via multi-view non-negative matrix factorization with local graph regularization. In: *2015 IEEE International Conference on Image Processing (ICIP)*, pp 3500–3504
- Yu X, Yu G, Wang J, Domeniconi C (2019) Co-clustering ensembles based on multiple relevance measures. *IEEE Transactions on Knowledge and Data Engineering* pp 1–1, DOI 10.1109/TKDE.2019.2942029